Autonomic Neuroscience: Basic and Clinical 142 (2008) 77–81

Contents lists available at ScienceDirect

Autonomic Neuroscience: Basic and Clinical

journal homepage: www.elsevier.com/locate/autneu

Activation of Rho-kinase in the brainstem enhances sympathetic drive in mice with heart failure

Koji Ito [1], Yoshikuni Kimura [1], Yoshitaka Hirooka *, Yoji Sagara, Kenji Sunagawa

Department of Cardiovascular Medicine, Kyushu University Graduate School of Medical Sciences, Fukuoka, Japan

ARTICLE INFO

Article history:
Received 12 December 2007
Received in revised form 23 June 2008
Accepted 24 July 2008

Keywords:
Heart failure
Sympathetic nervous system
Brain
Rho

ABSTRACT

Rho-kinase is involved in the pathogenesis of hypertension and left ventricular remodelling after myocardial infarction (MI). In an earlier study, we had demonstrated that Rho-kinase in the brainstem contributes to hypertensive mechanisms via the sympathetic nervous system; however, it is not known whether Rho-kinase in the brainstem also contributes to sympathetic nerve activation after MI.

Male Institute of Cancer Research mice (8–10 weeks old) were used for the study. Two days before coronary artery occlusion (MI group), the left ventricular function was estimated by echocardiography. Following this, Y-27632 (0.5 mM, 0.25 μL/h), a specific Rho-kinase inhibitor, or a vehicle was intracisternally infused in the mice using an osmotic mini-pump. Nine days after coronary artery occlusion, we evaluated the 24-hour urinary norepinephrine excretion (U-NE) as a marker of sympathetic nerve activity. Ten days after coronary artery occlusion, we measured organ weight and evaluated Rho-kinase activity in the brainstem by measuring the amount of phosphorylated ezrin/radixin/moesin proteins, one of the substrates of Rho-kinase. The control group underwent a sham operation. Rho-kinase activity, U-NE, and lungs and liver weight were significantly greater in the MI group compared with the control group. Left ventricular size increased and percent fractional shortening decreased in the MI group compared with the control group. Y-27632 significantly decreased Rho-kinase activity and attenuated the increase in U-NE after MI.

These results demonstrate that Rho-kinase is activated in the brainstem after MI and that the activation of this pathway is involved in the resulting enhanced sympathetic drive.

1. Introduction

Patients with heart failure present with a variety of physiologic abnormalities, including high levels of sympathetic nerve activity (Mark, 1995; Zucker et al., 1995; Middlekauff and Mark, 1998). The sympathetic nervous system is activated early in the course of heart failure (Francis et al., 1990), and sympathetic and humoral activation precede the onset of clinically recognizable heart failure (Benedict et al., 1996). Sympathetic nerve activation, which changes to adjust to a reduction in cardiac function, also contributes to the adverse outcomes of decompensated heart failure. In fact, accumulating evidence indicates that β-blockers are one of the most effective drugs for the treatment of patients with chronic heart failure (Waagstein et al., 1993; Bristow et al., 1994; Packer et al., 1996). Furthermore, plasma norepinephrine levels increase and correlate with mortality in patients with heart failure (Cohn et al., 1984; Rector et al., 1987). Based on these observations, it can be concluded that activation of the sympathetic nervous system plays an important role in the progression of heart failure; however, the detailed mechanisms of this process are not clear. Therefore, studies of the pathophysiology of heart failure have extensively focused on sympathetic nervous system activation.

The brainstem has several cardiovascular centres, such as the nucleus tractus solitarius (NTS), caudal ventrolateral medulla (CVLM), and rostral ventrolateral medulla (RVLM; Dampney et al., 1994). In recent articles, we had reported that activation of the Rho/Rho-kinase pathway in the brainstem contributes to hypertensive mechanisms and baroreflex dysfunction, in several hypertensive models, via the sympathetic nervous system (Ito et al., 2003, 2004a,b, 2005a,b, 2006). It is not known, however, whether this pathway is involved in the enhanced sympathetic nervous system activity associated with heart failure. Therefore, the aim of this study was to determine whether the activation of the Rho/Rho-kinase pathway in the brainstem contributes to enhanced sympathetic nerve activity in heart failure. For this purpose, we evaluated Rho-kinase activity in the brainstem of mice with heart failure (myocardial infarction [MI]) after left coronary artery (LCA) occlusion. Furthermore, we examined the effects of an intracisternal infusion of a Rho-kinase inhibitor on sympathetic nerve activation in mice with heart failure.

* Corresponding author. Department of Cardiovascular Medicine, Kyushu University Graduate School of Medical Sciences, 3-1-1 Maidashi, Higashi-ku, Fukuoka 812-8582, Japan. Tel.: +81 92 642 5360; fax: +81 92 642 5374.
E-mail address: hyoshi@cardiol.med.kyushu-u.ac.jp (Y. Hirooka).

[1] These authors equally contributed to this study.

1566-0702/$ – see front matter © 2008 Elsevier B.V. All rights reserved.
doi:10.1016/j.autneu.2008.07.010

2. Materials and methods

2.1. Animals

The study was reviewed and approved by the Committee on Ethics of Animal Experiments, Kyushu University Graduate School of Medical Sciences, and was conducted according to the Guidelines for Animal Experiments of Kyushu University. Male Institute of Cancer Research (ICR) mice (8–10 weeks old; SLC, Fukuoka, Japan) were used.

2.2. Mouse heart failure model preparation

The mice underwent LCA occlusion to produce MI (MI group). The surgical procedures are described in detail elsewhere (Michael et al., 1995). Briefly, after sodium pentobarbital anaesthesia (25–40 mg/kg intraperitoneally) and intubation with a polyethylene tube, the animals were ventilated using a volume-cycled rodent respirator with a 2–3 mL/cycle and at a respiratory rate of 120 breaths/min. After thoracotomy, the LCA was ligated with a suture 3–4 mm from the tip of the left auricle. The chest wall and skin were then closed with sutures. A sham operation (without LCA occlusion) was similarly performed on the control group (sham-operated group).

The resultant infarcts were evaluated using serial 5-μm sections stained with Masson's trichrome stain. Infarct length was measured along the endocardial and epicardial surfaces from the LV sections. Total LV circumference was calculated as the sum of endocardial and epicardial segment lengths. Infarct size was calculated as the infract circumference divided by the total circumference times 100.

2.3. Echocardiographic imaging

Just before and ten days after LCA occlusion, serial M-mode echocardiographies were performed on all animals under light sodium pentobarbital anaesthesia with spontaneous respiration. An echocardiography system (SSD5000; Aloka, Tokyo, Japan) with a dynamically focused 7.5-MHz linear array transducer was used. M-mode tracings were recorded from the short-axis view at the level of the papillary muscle. LV end-diastolic diameter (LVEDD), LV end-systolic diameter (LVESD) and wall thickness were measured. Percent fractional shortening (%FS) was calculated as follows: $\%FS = (LVEDD) - (LVESD)/(LVEDD) \times 100$.

2.4. Continuous intracisternal infusion with a Rho-kinase inhibitor

Two days before LCA occlusion, the mice were anaesthetized with sodium pentobarbital (50 mg/kg intraperitoneally). An osmotic mini-pump – filled with a vehicle (artificial cerebrospinal fluid containing 123 mM NaCl, 0.86 mM $CaCl_2$, 3.0 mM KCl, 0.89 mM $MgCl_2$, 25 mM $NaHCO_3$, 0.5 mM NaH_2PO_4 and 0.25 mM Na_2HPO_4; pH 7.4) or with Y-27632 dissolved in artificial cerebrospinal fluid – was subcutaneously implanted in the dorsum of each of the mice and connected to a polyethylene tube (PE-10). The osmotic mini-pump infusion rate was 0.25 μL/h and the pumps were calibrated to empty after 14 days. A small hole was made in the atlantooccipital membrane, which covers the dorsal surface of the medulla, and the tip of the tube was placed intracisternally and fixed in place with tissue adhesive.

2.5. Measurement of blood pressure and heart rate

At day 10 after the interventions (LCA occlusion and sham operation), the systolic blood pressure and heart rate were measured using the tail-cuff method in an awake state.

2.6. Evaluation of Rho-kinase activity

At day 10 after the interventions (LCA occlusion and sham operation), the animals were sacrificed using an overdose of sodium pentobarbital and brainstem tissues were obtained. The tissues were homogenized in a lysing buffer containing 40 mmol/L HEPES (4-[2-hydroxyethyl]-1-piperazineethanesulfonic acid), 1% Triton® X-100, 10% glycerol, 1 mmol/L Na_3VO_4 (sodium orthovanadate) and 1 mmol/L phenylmethylsulfonyl fluoride. The tissue lysate was centrifuged and the supernatant collected. The protein concentration was determined using a BCA (bicinchoninic acid) protein assay kit (Pierce Chemical Co., Rockford, IL). An aliquot part of 15 μg of protein from each sample was separated on 10% sodium dodecyl sulfate–polyacrylamide gel. The proteins were subsequently transferred onto polyvinylidene difluoride (PVDF) membranes (Immobilon®-P membrane; Millipore, Billerica, MA). Membranes were incubated with goat immunoglobin G (IgG) monoclonal antibody to Rho-kinase (ROCK-2; 1:1000, Santa Cruz Biotechnology, CA), with rabbit IgG polyclonal antibody to RhoA (1:1000, Santa Cruz Biotechnology) or with rabbit anti-phosphorylated ERM family members – ezrin (Thr567), radixin (Thr564) and moesin (Thr558) – which are target proteins of Rho-kinase (Matsui et al., 1998). Membranes were then incubated with a horseradish peroxidase-conjugated horse anti-goat or rabbit IgG antibody (1:10,000). Rabbit IgG polyclonal antibody to β-tubulin (1:5000, Santa Cruz Biotechnology) for the brain tissues was used as an internal control. Immunoreactivity was detected by enhanced chemiluminescence autoradiography (ECL™ Western blotting detection kit; Amersham Pharmacia Biotech, Uppsala, Sweden), and the film was analyzed using NIH Image.

2.7. Measurement of organ weight

When the mice were sacrificed, the liver and lungs were also removed and weighed.

2.8. Measurement of urinary norepinephrine excretion

The 24-hour urinary norepinephrine (U-NE) excretion was measured by high-performance liquid chromatography two days before and nine days after LCA occlusion.

2.9. Statistics

All values are expressed as mean ± S.E. An unpaired *t*-test was used to compare values between the MI mice and sham-operated mice. A paired *t*-test was used to compare the values before and after each operation in the sham-operated mice and MI mice. A two-way ANOVA was used to compare the LVEDD and %FS between the MI group infused with the vehicle (MI + vehicle group) and the MI group infused with Y-27632 (MI + Y-27632 group). Differences were considered to be significant when $P < 0.05$.

3. Results

3.1. Heart failure characteristics

Systolic blood pressure and heart rate did not significantly alter after MI. The weight of the liver and lungs significantly increased in

Table 1
Physiological parameters of each group

	Sham ($n=10$)	MI + vehicle ($n=9$)	MI + Y-27632 ($n=10$)
Body weight (g)	43 ± 3	40 ± 5	39 ± 4
Lung (mg)/BW(g)	5.7 ± 0.1	7.2 ± 0.2*	6.8 ± 0.2*
Liver (mg)/BW(g)	6.8 ± 0.7	8.8 ± 0.4*	7.7 ± 0.3*
Heart (mg)/BW(g)	3.6 ± 0.1	4.0 ± 0.4	3.9 ± 0.3
SBP (mm Hg)	124 ± 15	126 ± 12	118 ± 11
HR (bpm)	422 ± 33	442 ± 28	398 ± 30

Values are means ± S.E; *n*, number of mice.
* $P < 0.05$ versus sham group.

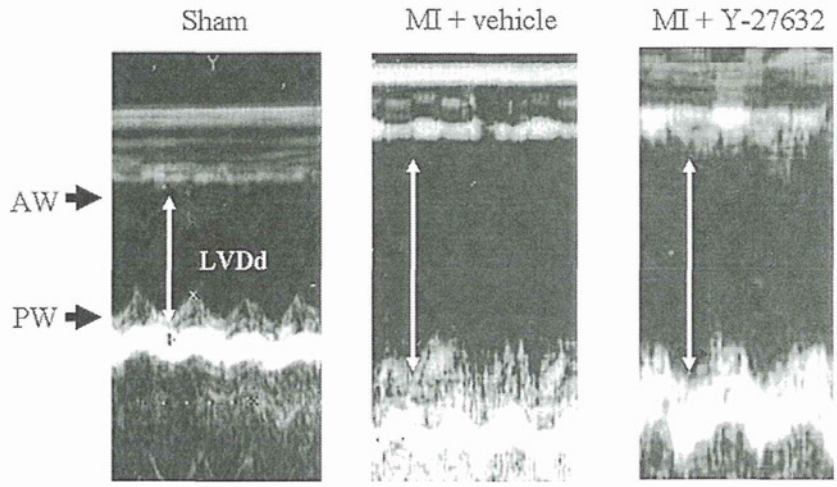

Fig. 1. M-mode echocardiograms of the left ventricle in parasternal short-axis view obtained from the sham-operated group, the myocardial infarction group with the vehicle (MI+vehicle) and the myocardial infarction group with Y-27632 (MI+Y-27632). LVEDd: left ventricular end-diastolic diameter; AW: anterior wall; PW: posterior wall.

the MI group compared with the sham-operated group (Table 1). Infarct size did not differ between the MI+vehicle group and MI+Y-27632 group (55±3% versus 55±2%). Echocardiographic evaluation revealed that the LVEDD was larger and %FS was smaller in the MI group than in the sham-operated group (Fig. 1, Table 2). Furthermore, the 24-hour U-NE excretion was significantly higher in the MI group compared with the sham-operated group (Fig. 2).

3.2. Effects of Rho-kinase inhibition in the brainstem on heart failure characteristics

Intracisternal infusion of Rho-kinase inhibitor Y-27632 significantly attenuated the increases in 24-hour U-NE excretion in the MI group to levels similar to those of before the LCA occlusion, indicating that intracisternal infusion of Y-27632 prevented the increase in sympathetic nerve activation in the MI group (Fig. 2). The echocardiographic values and organ weights did not differ statistically between the MI+Y-27632 group and MI+vehicle group (Tables 1 and 2). Although systolic blood pressure and heart rate also did not significantly differ between the MI+vehicle group and MI+Y-27632 group, heart rate tended to decrease in the MI+Y-27632 group compared with the MI+vehicle group ($p=0.1$; Table 1).

In the sham-operated group ($n=4$), Y-27632 did not affect the systolic blood pressure (125±11 mm Hg), heart rate (414±20 bpm) or U-NE excretion (Fig. 2).

3.3. RhoA and Rho-kinase protein expression and Rho-kinase activity in brainstem

The levels of RhoA and Rho-kinase proteins did not change in any group (Fig. 3). However, the levels of phosphorylated ezrin/radixin/moesin (p-ERM) proteins, which indicate Rho-kinase activity, were higher in the MI group compared with the sham-operated group (Fig. 3). Intracisternal infusion of Y-27632 significantly attenuated the expression level of p-ERM proteins in the MI group to levels similar to those of the sham-operated group (Fig. 3).

Table 2
Echocardiographic parameters of each group

	Sham ($n=10$)	MI+vehicle ($n=9$)	MI+Y-27632 ($n=10$)
LVDd (mm)	3.4±0.3	4.1±0.1*	3.8±0.5*
LVDs (mm)	2.1±0.1	2.5±0.1*	2.2±0.4*
FS (%)	39±2	17±1*	18±1*

Value are means±S.E; *n*, number of mice; LVEDD, left ventricular end-diastolic dimension; LVESD, left ventricular end-systolic dimension; %FS, percent fractional shortening.
* $P<0.05$ versus sham group.

4. Discussion

The major finding in this study was that the Rho/Rho-kinase pathway in the brainstem contributes to the activation of the sympathetic nervous system in mice with heart failure after MI. U-NE and Rho-kinase activity were increased in the brainstem of these mice. Inhibition of Rho-kinase activity in the brainstem by intracisternal infusion of Y-27632 significantly reduced U-NE. These findings suggest that increased Rho-kinase activity in the brainstem contributes to the sympathetic hyperactivation in mice with heart failure after MI.

In the mice, heart failure was produced by LCA occlusion. The resulting LV dilatation and reduced LV systolic function were confirmed by echocardiography. Also, U-NE, a marker of sympathetic nerve activity, was significantly increased in the MI mice. Heart failure is characterized by an enhanced sympathetic drive in experimental animals as well as in patients (Mark, 1995; Zucker et al., 1995; Middlekauff and Mark, 1998). In patients with heart failure, plasma norepinephrine levels increase with the severity of heart failure. Furthermore, in heart failure, the weight of the lungs and liver increases due to congestion. In this study, we confirmed that the weight of the lungs and liver significantly increased in the MI mice

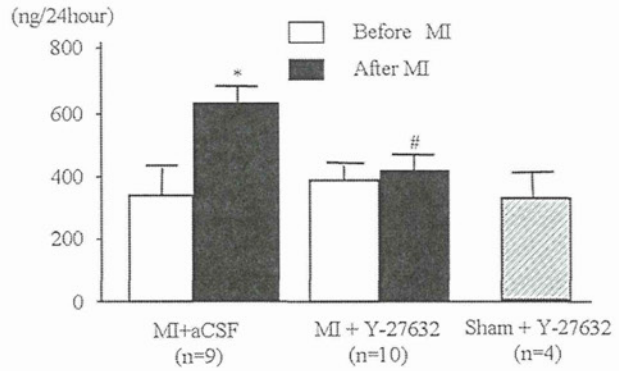

Fig. 2. The 24-hour urinary norepinephrine (U-NE) excretion in each group (*$P<0.05$ versus before myocardial infarction [MI], #$P<0.05$ versus myocardial infarction group with the vehicle [MI+vehicle]).

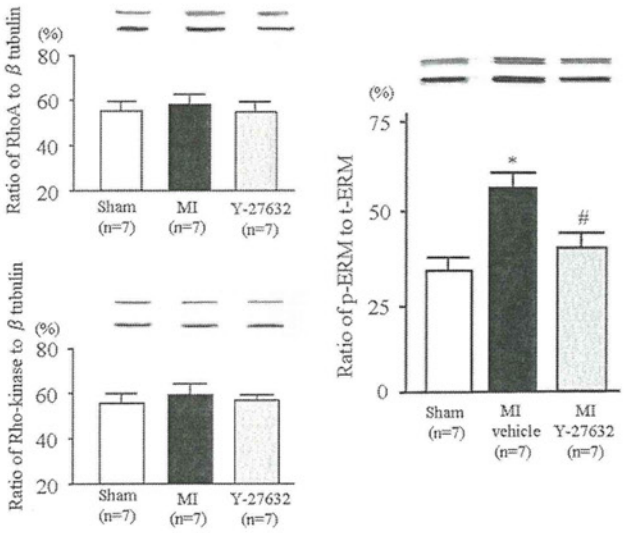

Fig. 3. Left: Level of RhoA and Rho-kinase protein in the brainstem in each group. Right: Level of phosphorylated ezrin/radixin/moesin (p-ERM) family, a target protein of Rho-kinase, in the brainstem in each group (*$P<0.05$ versus sham-operated group, #$P<0.05$ versus myocardial infarction group with the vehicle [MI+vehicle]).

compared with the sham-operated mice. These results indicate that the MI mice were in a heart failure state, validating the use of these mice as a heart failure model.

In recent studies, we had demonstrated that the Rho/Rho-kinase pathway in the brainstem is involved in blood pressure regulation and baroreflex function via the sympathetic nervous system, and activation of this pathway contributes to the central hypertensive mechanisms of several hypertensive models (Ito et al., 2003, 2004a, 2005a,b, 2006). The Rho/Rho-kinase pathway is activated by angiotensin II (Sagara et al., 2007; Funakoshi et al., 2001), and angiotensin II may have an important role in sympathetic nerve activation of heart failure (Felder et al., 2001; Shigematsu et al., 2001; Zucker, 2006). Further, an increase in angiotensin II may be necessary for sustained sympathetic hyperactivation in heart failure (Liu and Zucker, 1999). Inhibition of angiotensin II type1 receptors in the NTS reduces blood pressure, heart rate, and sympathetic nerve activity in rats with chronic inhibition of nitric oxide synthase (Eshima et al., 2000). Therefore, we hypothesized that the Rho/Rho-kinase pathway in the brainstem contributes to sympathetic nerve activation in mice with heart failure after MI, and we evaluated the role of this pathway in the brainstem in sympathetic hyperactivation.

The finding that the increase in U-NE in the MI mice was significantly reduced by an intracisternal infusion of Y-27632 was most important in this study, and this finding indicates that the Rho/Rho-kinase pathway in the brainstem contributes to the increase in sympathetic nerve activity after MI. We evaluated sympathetic nerve activity by the U-NE, which may be dependent on renal function. Although we did not assess this issue, the criterion of using U-NE for the estimation of sympathetic nerve activity in heart failure models has already been established (Sakai et al., 2005). Furthermore, the aim of our study was to compare the effects of Rho-kinase inhibition on the sympathetic nerve activity between the MI+Y-27632 group and MI+vehicle group. Therefore, we measured the U-NE excretion as a marker of sympathetic nerve activity.

The mechanisms of blood pressure regulation by Rho-kinase have not been fully understood. Inhibition of Rho-kinase enhances glutamate sensitivity in excitatory synapses, such as in the NTS (Ito et al., 2005a). Whether this mechanism contributed to the reduced sympathetic nerve activity caused by Y-27632 in the MI mice remains unknown. A study has reported that the Rho/Rho-kinase pathway negatively regulates endothelial nitric oxide synthase (NOS) expression (Laufs and Liao, 1998). Also, nitric oxide in the brain inhibits sympathetic nerve activity (Sakai et al., 2000; Kishi et al., 2001, 2002). In fact, a recent study demonstrated that NOS expression in the brainstem, especially in the NTS, is reduced in an MI mouse model of heart failure, and up-regulation of NOS in the NTS attenuates the enhanced sympathetic drive (Sakai et al., 2005). Therefore, attenuation of the sympathetic drive by intracisternal infusion of Y-27632 might be by an effect of nitric oxide.

We evaluated the Rho-kinase activity using the p-ERM levels as one of the markers. Other target proteins, such as adducin and cofilin, might also have been phosphorylated by Rho-kinase, and the levels of these proteins could have changed. In fact, in an earlier study, we had demonstrated that phosphorylated adducin (p-adducin) levels also increased in the brainstem of spontaneously hypertensive rats compared with Wistar–Kyoto rats (Ito et al., 2003).

As seen from the results of earlier studies (Funakoshi et al., 2001; Matsumoto et al., 2008), factors such as angiotensin II and endothelin also play a role in activating the Rho/Rho-kinase pathway. Also, in previous studies, we had reported that central angiotension II produced pressor responses by the activation of Rho-kinase in the brainstem (Sagara et al., 2007), and that in the heart failure model, the renin–angiotensin system (RAS) was activated in the brainstem (Shigematsu et al., 2001). Therefore, RAS might be one of the mechanisms for Rho-kinase stimulation in heart failure. However, we have not addressed these issues in this study. Further research is needed to confirm these hypotheses.

5. Study limitations

Intracisternal infusion of Y-27632 might affect many areas of the brain, including the cardiovascular centre, and it is not possible to identify specific areas affected by intracisternally infused drugs. Intracisternal infusion of Y-27632 might also alter neuronal activity in areas other than in the NTS, such as in the RVLM, due to the flow of cerebrospinal fluid. Therefore, we examined Rho-kinase activity in the whole brainstem for this study. As we had previously demonstrated that Y-27632 has greater effects on blood pressure when injected into the NTS rather than into the RVLM of rats (Ito et al., 2005b), we speculate that intracisternal infusion of Y-27632 alters neuronal activity mainly in the NTS. However, we could not confirm this speculation because of the technical difficulties involved in using mice as experimental animals.

In this study, we did not find an improvement in cardiac function despite the attenuation of sympathetic nerve activation by the Rho-kinase inhibitor. These results might be attributed to the brief treatment and survey duration. In fact, LV dimensions tended to decrease in the MI+Y-27632 group rather than in the MI+vehicle group. Thus, if we had treated the MI group with Y-27632 for a much longer period, it might have been possible to detect a significant improvement in cardiac function. Therefore, further study is needed to evaluate the long-term effects of Rho-kinase inhibition on improvement of cardiac function or on survival.

6. Conclusion

After MI, the mice showed characteristics consistent with those of heart failure. From the enhanced sympathetic nerve activity observed, it can be concluded that this enhancement is mediated by Rho-kinase in the brainstem. In addition, treatment with a Rho-kinase inhibitor before LCA occlusion might have preventive effects on heart failure deterioration.

Acknowledgements

This study was supported by Grants-in-Aid for Scientific Research from the Japan Society for the Promotion of Science.

References

Benedict, C.R., Shelton, B., Johnstone, D.E., Francis, G., Greenberg, B., Konstam, M., Probstfield, J.L., Yusuf, S., 1996. Prognostic significance of plasma norepinephrine in patients with asymptomatic left ventricular dysfunction. Circulation 94, 690–697.

Bristow, M.R., O'Connell, J.B., Gilbert, E.M., French, W.J., Leathermen, G., Kantrowitz, N.E., Orie, J., Smucker, M.L., Marshall, G., Kelly, P., 1994. Dose-response of chronic beta-blocker treatment in heart failure from either idiopathic dilated or ischemic cardiomyopathy. Circulation 89, 1632–1642.

Cohn, J.N., Levine, T.B., Olivari, M.T., Garberg, V., Lura, D., Francis, G.S., Simon, A.B., Rector, T., 1984. Plasma norepinephrine as a guide to prognosis in patients with chronic congestive heart failure. N. Engl. J. Med. 311, 819–823.

Dampney, R.A.L., Polson, J.W., Potts, P.D., Hirooka, Y., 1994. Functional organization of central pathway regulating the cardiovascular system. Physiol. Rev. 74, 323–364.

Eshima, K., Hirooka, Y., Shigematsu, H., Matsuo, I., Koike, G., Sakai, K., Takeshita, A., 2000. Angiotensin II in the nucleus tractus solitarii contributes to neurogenic hypertension caused by chronic nitric oxide synthase inhibition. Hypertension 36, 259–263.

Felder, R.B., Francis, J., Weiss, R.M., Zhang, Z.H., Wei, S.G., Johnson, A.K., 2001. Neurohumoral regulation in ischemia-induced heart failure. Role of the forebrain. Ann. N.Y. Acad. Sci. 940, 444–453.

Francis, G.S., Benedict, C., Johnstone, D.E., Kirlin, P.C., Nicklas, J., Liang, C.S., Kubo, S.H., Rudin-Toretsky, E., Yusuf, S., 1990. Comparison of neuroendocrine activation in patients with left ventricular dysfunction with and without congestive heart failure. A substudy of the Studies of Left Ventricular Dysfunction (SOLVD). Circulation 82, 1724–1729.

Funakoshi, Y., Ichiki, T., Shimokawa, H., Egashira, K., Takeda, K., Kaibuchi, K., Takeya, M., Yoshimura, T., Takeshita, A., 2001. A critical role of Rho-kinase in angiotensin II-induced monocyte chemoattractant protein-1 expression in rat vascular smooth muscle cells. Hypertension 38, 100–104.

Ito, K., Hirooka, Y., Sakai, K., Kishi, T., Kaibuchi, K., Shimokawa, H., Takeshita, A., 2003. Rho/Rho-kinase pathway in brainstem contributes to blood pressure regulation via sympathetic nervous system; possible involvement in neural mechanisms of hypertension. Circ. Res. 92, 1337–1343.

Ito, K., Hirooka, Y., Kishi, T., Kimura, Y., Kaibuchi, K., Shimokawa, H., Takeshita, A., 2004a. Rho/Rho-kinase pathway in the brainstem contributes to hypertension caused by chronic nitric oxide synthase inhibition. Hypertension 43, 156–162.

Ito, K., Hirooka, Y., Sagara, Y., Kimura, Y., Kaibuchi, K., Shimokawa, H., Takeshita, A., Sunagawa, K., 2004b. Inhibition of Rho-kinase in the brainstem augments baroreflex control of heart rate in rats. Hypertension 44, 478–483.

Ito, K., Hirooka, Y., Hori, N., Kimura, Y., Sagara, Y., Shimokawa, H., Takeshita, A., Sunagawa, K., 2005a. Inhibition of Rho-kinase in the nucleus tractus solitarius enhances glutamate sensitivity in rats. Hypertension 46, 360–365.

Ito, K., Hirooka, Y., Kimura, Y., Shimokawa, H., Takeshita, A., 2005b. Effects of hydroxyfasudil administered to the nucleus tractus solitarii on blood pressure and heart rate in spontaneously hypertensive rats. Clin. Exp. Hypertens. 2, 269–277.

Ito, K., Hirooka, Y., Kimura, Y., Sagara, Y., Sunagawa, K., 2006. Ovariectomy augments hypertension through Rho-kinase activation in the brain stem in female spontaneously hypertensive rats. Hypertension 48, 651–657.

Kishi, T., Hirooka, Y., Sakai, K., Shigematsu, H., Shimokawa, H., Takeshita, A., 2001. Overexpression of eNOS in the RVLM causes hypotension and bradycardia via GABA release. Hypertension 38, 896–901.

Kishi, T., Hirooka, Y., Ito, K., Sakai, K., Shimokawa, H., Takeshita, A., 2002. Cardiovascular effects of overexpression of endothelial nitric oxide synthase in the rostral ventrolateral medulla in stroke-prone spontaneously hypertensive rats. Hypertension 39, 264–268.

Laufs, U., Liao, J.K., 1998. Post-transcriptional regulation of endothelial nitric oxide synthase mRNA stability by Rho GTPase. J. Biol. Chem. 273, 24266–24271.

Liu, J.L., Zucker, I.H., 1999. Regulation of sympathetic nerve activity in heart failure: a role for nitric oxide and angiotensin II. Circ. Res. 94, 402–423.

Mark, A.L., 1995. Sympathetic dysregulation in heart failure: mechanisms and therapy. Clin. Cardiol. 18, I3–I8.

Matsui, T., Maeda, M., Doi, Y., Yonemura, S., Amano, M., Kaibuchi, K., Tsukita, S., 1998. Rho-kinase phosphorylates COOH-terminal threonines of ezrin/radixin/moesin (ERM) proteins and regulates their head-to-tail association. J. Cell Biol. 140, 647–657.

Matsumoto, T., Kakami, M., Kobayashi, T., Kamata, K., 2008. Gender differences in vascular reactivity to endothelin-1 (1-31) in mesenteric arteries from diabetic mice. Peptides 29, 1338–1346.

Michael, L.H., Entman, M.L., Hartley, C.J., Youler, K.A., Zhu, J., Hall, S.R., Hawkins, H.K., Berens, K., Ballantyne, C.M., 1995. Myocardial ischemia and reperfusion: a murine model. Am. J. Physiol. 269, H2147–H2154.

Middlekauff, H.R., Mark, A.L., 1998. The treatment of heart failure: the role of neurohumoral activation. Intern. Med. 37, 112–122.

Packer, M., Bristow, M.R., Cohn, J.N., Colucci, W.S., Fowler, M.B., Gilbert, E.M., Shusterman, N.H., 1996. The effect of carvedilol on morbidity and mortality in patients with chronic heart failure. U.S. Carvedilol Heart Failure Study Group. N. Engl. J. Med. 334, 1349–1355.

Rector, T.S., Olivari, M.T., Levine, T.B., Francis, G.S., Cohn, J.N., 1987. Predicting survival for an individual with congestive heart failure using the plasma norepinephrine concentration. Am. Heart J. 114, 148–152.

Sagara, Y., Hirooka, Y., Nozoe, M., Ito, K., Kimura, Y., Sunagawa, K., 2007. Pressor responses induced by central angiotensin II is mediated by activation of Rho/Rho-kinase pathway via AT1 receptors. J. Hypertens. 25, 399–406.

Sakai, K., Hirooka, Y., Matsuo, I., Eshima, K., Shigematsu, H., Shimokawa, H., Takeshita, A., 2000. Overexpression of eNOS in NTS causes hypotension and bradycardia in vivo. Hypertension 36, 1023–1028.

Sakai, K., Hirooka, Y., Shigematsu, H., Kishi, T., Ito, K., Shimokawa, H., Takeshita, A., Sunagawa, K., 2005. Overexpression of eNOS in brain stem reduces enhanced sympathetic drive in mice with myocardial infarction. Am. J. Physiol. Heart Circ. Physiol. 289, H2159–H2166.

Shigematsu, H., Hirooka, Y., Eshima, K., Shihara, M., Tagawa, T., Takeshita, A., 2001. Endogenous angiotensin II in the NTS contributes to sympathetic activation in rats with aortocaval shunt. Am. J. Physiol. 280, 1665–1673.

Waagstein, F., Bristow, M.R., Swedberg, K., Camerini, F., Fowler, M.B., Silver, M.A., Gilbert, E.M., Johnson, M.R., Goss, F.G., Hjalmarson, A., 1993. Beneficial effects of metoprolol in idiopathic dilated cardiomyopathy. Metoprolol in Dilated Cardiomyopathy (MDC) Trial Study Group. Lancet 342, 1441–1446.

Zucker, I.H., 2006. Novel mechanisms of sympathetic regulation in chronic heart failure. Hypertension 48, 1005–1011.

Zucker, I.H., Wang, W., Brandle, M., Schultz, H.D., Patel, K.P., 1995. Neural regulation of sympathetic nerve activity in heart failure. Prog. Cardiovasc. Dis. 37, 397–414.

Am J Physiol Heart Circ Physiol 295: H1855–H1866, 2008.
First published August 29, 2008; doi:10.1152/ajpheart.522.2008.

Contrasting effects of presynaptic α_2-adrenergic autoinhibition and pharmacologic augmentation of presynaptic inhibition on sympathetic heart rate control

Tadayoshi Miyamoto,[1,2] Toru Kawada,[2] Yusuke Yanagiya,[2] Tsuyoshi Akiyama,[3] Atsunori Kamiya,[2] Masaki Mizuno,[2] Hiroshi Takaki,[2] Kenji Sunagawa,[4] and Masaru Sugimachi[2]

[1]*Department of Physical Therapy, Faculty of Health Sciences, Morinomiya University of Medical Sciences; and* [2]*Department of Cardiovascular Dynamics, Advanced Medical Engineering Center, and* [3]*Department of Cardiac Physiology, National Cardiovascular Center Research Institute, Osaka; and* [4]*Department of Cardiovascular Medicine, Graduate School of Medical Sciences, Kyusyu University, Fukuoka, Japan*

Submitted 16 May 2008; accepted in final form 19 August 2008

Miyamoto T, Kawada T, Yanagiya Y, Akiyama T, Kamiya A, Mizuno M, Takaki H, Sunagawa K, Sugimachi M. Contrasting effects of presynaptic α_2-adrenergic autoinhibition and pharmacologic augmentation of presynaptic inhibition on sympathetic heart rate control. *Am J Physiol Heart Circ Physiol* 295: H1855–H1866, 2008. First published August 29, 2008; doi:10.1152/ajpheart.522.2008.—Presynaptic α_2-adrenergic receptors are known to exert feedback inhibition on norepinephrine release from the sympathetic nerve terminals. To elucidate the dynamic characteristics of the inhibition, we stimulated the right cardiac sympathetic nerve according to a binary white noise signal while measuring heart rate (HR) in anesthetized rabbits ($n = 6$). We estimated the transfer function from cardiac sympathetic nerve stimulation to HR and the corresponding step response of HR, with and without the blockade of presynaptic inhibition by yohimbine (1 mg/kg followed by 0.1 $mg \cdot kg^{-1} \cdot h^{-1}$ iv). We also examined the effect of the α_2-adrenergic receptor agonist clonidine (0.3 and 1.5 $mg \cdot kg^{-1} \cdot h^{-1}$ iv) in different rabbits ($n = 5$). Yohimbine increased the maximum step response (from 7.2 ± 0.8 to 12.2 ± 1.7 beats/min, means ± SE, $P < 0.05$) without significantly affecting the initial slope (0.93 ± 0.23 vs. 0.94 ± 0.22 $beats \cdot min^{-1} \cdot s^{-1}$). Higher dose but not lower dose clonidine significantly decreased the maximum step response (from 6.3 ± 0.8 to 6.8 ± 1.0 and 2.8 ± 0.5 beats/min, $P < 0.05$) and also reduced the initial slope (from 0.56 ± 0.07 to 0.51 ± 0.04 and 0.22 ± 0.06 $beats \cdot min^{-1} \cdot s^{-1}$, $P < 0.05$). Our findings indicate that presynaptic α_2-adrenergic autoinhibition limits the maximum response without significantly compromising the rapidity of effector response. In contrast, pharmacologic augmentation of the presynaptic inhibition not only attenuates the maximum response but also results in a sluggish effector response.

systems analysis; transfer function; α-adrenergic blockade; rabbits

PRESYNAPTIC α_2-ADRENERGIC receptors play an important role in regulating neurotransmitter release in the central and peripheral nervous systems. The concept that neurotransmitter release is modulated by presynaptic autoreceptors was proposed in the 1970s (19, 20, 25, 31–33, 37, 38). Langer (18) first demonstrated that an α-adrenergic antagonist phentolamine, at a concentration below that required to produce its negative chronotropic effect, increases the magnitude of heart rate (HR) response to sympathetic nerve stimulation. Since then, a number of in vivo and in vitro studies have been conducted to characterize the negative feedback regulation of norepinephrine (NE) release via the presynaptic α_2-adrenergic receptors located on the sympathetic nerve terminals (1, 6, 9, 11, 17, 24, 26, 27a, 29, 30, 34, 35). However, the dynamic nature of the presynaptic α_2-adrenergic inhibition in sympathetic HR control remains to be quantified. Because we focus on the effector response to sympathetic nerve stimulation, the term "presynaptic" may be interpreted as "prejunctional" throughout this paper to describe more specifically the NE kinetics at the neuroeffector junction.

We first schematize our hypothesis on the possible modes of operations of the presynaptic inhibition. With reference to Fig. 1, the solid and dotted lines indicate the HR responses with and without the presynaptic inhibition, respectively. Figure 1*A* represents a "limiter-like" operation of the presynaptic inhibition in which the steady-state response is attenuated, while the initial slope of the response is unchanged. Figure 1*B* represents an "attenuator-like" operation in which the steady-state response is attenuated, while the initial slope of the response is also reduced in proportion to the attenuation of the steady-state response. Since the rapid effector response is one of the important hallmarks of neural regulation compared with humoral regulation, determining which of the two operations likely occurs would contribute to the physiological understanding of the presynaptic inhibition. The words "limiter-like" and "attenuator-like" in this paper are used in the specific senses described above.

To answer which of the two operations likely occurs in the presynaptic inhibition, we examined the HR response to dynamic sympathetic nerve stimulation, with or without blocking the α_2-adrenergic receptors in anesthetized rabbits. Because the HR response is mainly mediated by the postsynaptic β_1-adrenergic receptors, the administration of an α_2-adrenergic receptor antagonist does not eliminate the HR response to sympathetic nerve stimulation. We also examined the effects of pharmacologic augmentation of the α_2-adrenergic receptors on the HR response to dynamic sympathetic nerve stimulation. The results of the present study indicated that the presynaptic α_2-adrenergic autoinhibition is a limiter-like operation. In contrast, the pharmacologic

Address for reprint requests and other correspondence: T. Miyamoto, Dept. of Physical Therapy, Faculty of Health Sciences, Morinomiya Univ. of Medical Sciences, Osaka 559-8611, Japan (e-mail: miyamoto@morinomiya-u.ac.jp).

The costs of publication of this article were defrayed in part by the payment of page charges. The article must therefore be hereby marked "*advertisement*" in accordance with 18 U.S.C. Section 1734 solely to indicate this fact.

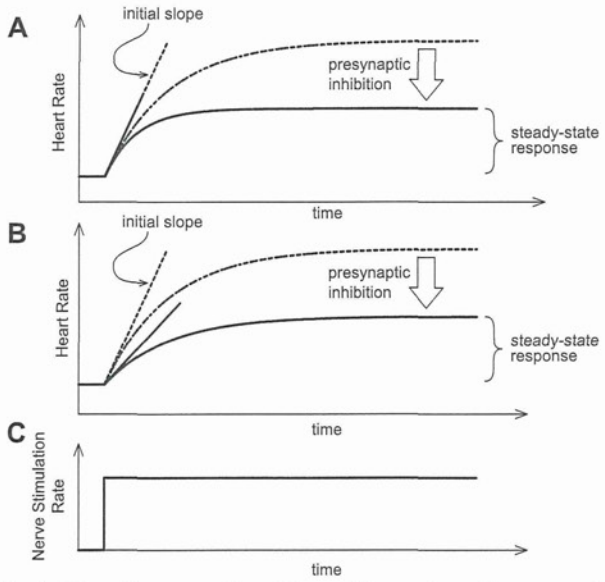

Fig. 1. Schematic representations of the possible operations of the presynaptic inhibition in heart rate (HR) step response to sympathetic nerve stimulation. The solid and dashed lines indicate the HR step response with and without the presynaptic inhibition, respectively. *A*: the presynaptic inhibition attenuates the steady-state response without affecting the initial slope of the response (a "limiter-like" operation). *B*: the presynaptic inhibition attenuates the steady-state response accompanied by a decrease in the initial slope in proportion to the attenuation of the steady-state response (an "attenuator-like" operation). Rapid effector response is maintained in the former but not in the latter. *C*: postulated nerve stimulation rate.

augmentation of presynaptic inhibition is an attenuator-like operation. A possible theoretical explanation for the difference in dynamic characteristics between the presynaptic α_2-adrenergic autoinhibition and the pharmacologic augmentation of the presynaptic inhibition will be proposed.

METHODS

Surgical Preparations

Animal care was in accordance with "Guiding Principles for the Care and Use of Animals in the Field of Physiological Sciences," approved by the Physiological Society of Japan. All protocols were reviewed and approved by the Animal Subject Committee of the National Cardiovascular Center. Japanese white rabbits, weighing 2.5–3.1 kg, were anesthetized by intravenous injection (2 ml/kg) of a mixture of urethane (250 mg/ml) and α-chloralose (40 mg/ml) and mechanically ventilated with oxygen-enriched room air. Tidal volume was set at 35 ml and the rate was adjusted between 35 and 40 cycles/min to be sufficient for suppressing spontaneous respiration. Supplemental doses of these anesthetics were administered by continuous intravenous infusion (1 $ml \cdot kg^{-1} \cdot h^{-1}$) into the marginal ear vein. Arterial pressure (AP) was monitored with a micromanometer catheter (model, Millar Instruments, Houston, TX) inserted into the right femoral artery. A catheter for drug administration was also placed in the right femoral vein. Sinoaortic denervation was performed bilaterally to minimize changes in systemic sympathetic activity via the arterial baroreflexes. The vagi were also sectioned bilaterally at the neck level to remove the vagal control on HR. The right inferior cardiac sympathetic nerve was exposed through a midline thoracotomy and sectioned. A pair of bipolar platinum electrodes was then attached to the cardiac end of the sectioned sympathetic nerve for stimulation (12, 13, 22, 23). The stimulation electrodes and nerve were secured with silicon glue (Kwik-Sil, World Precision Instruments, Sarasota, FL). Instantaneous HR was measured from the AP signal utilizing a cardiotachometer (Tachometer N4778, San-ei, Tokyo, Japan). Body temperature was maintained at 38°C with a heating pad throughout the experiment.

Experimental Procedures

Protocols. To estimate the transfer function from the sympathetic nerve stimulation to HR response, we employed a binary white noise stimulation signal with a switching interval of 5 s. The power spectrum of the sympathetic nerve stimulation rate was fairly constant up to 0.1 Hz and decreased to ~1/10 at 0.15 Hz. The upper frequency limit of the input power that covers the frequency range of physiological interest was determined based on our laboratory's previous studies (12, 23) and also preliminary experimental runs. Different sequences of binary white noise signals were used in different animals. Because HR is linearly related to cardiac output when stroke volume is unchanged, we chose HR as an output signal to understand sympathetic cardiovascular regulation. However, to rule out the possibility that the reciprocal relationship between R-R interval (RRI) and HR confounded the analytical results, we also calculated the transfer function using RRI as an output signal.

In *protocol 1* ($n = 6$), to examine the dynamic nature of the presynaptic α_2-adrenergic autoinhibition, we estimated the transfer function from dynamic sympathetic nerve stimulation to HR response from 20-min data obtained under control and α_2-adrenergic blockade conditions as follows. After recording the control data, an α_2-adrenergic antagonist yohimbine was administered intravenously with an initial bolus injection of 1 mg/kg, followed by continuous infusion at 0.1 $mg \cdot kg^{-1} \cdot h^{-1}$. The yohimbine bolus was equivalent to 10 h of infusion. The duration from the initiation of yohimbine administration until HR and AP reached new steady-state levels was ~15 min (35). We then repeated the 20-min dynamic sympathetic nerve stimulation and recorded the HR response under the α_2-adrenergic blockade condition.

In *protocol 2* ($n = 5$), to examine the effects of pharmacologic augmentation of the presynaptic α_2-adrenergic inhibition on the sympathetic HR control, we estimated the transfer function from dynamic sympathetic nerve stimulation to HR response before and during the administration of an α_2-adrenergic receptor agonist clonidine. Clonidine was administered intravenously at 0.3 and 1.5 $mg \cdot kg^{-1} \cdot h^{-1}$ in an increasing order. After 20-min baseline data collection, we started lower dose clonidine administration and waited for 15 min and then collected data for 20 min. Next, we started higher dose clonidine administration and waited for 15 min and then collected data for 20 min.

The stimulation rate of binary white noise was set at 0–1 Hz for *protocol 1*, and 0–5 Hz for *protocol 2*. Because we expected that blockade of the presynaptic α_2-adrenergic inhibition would augment, whereas activation of the inhibition would attenuate, the HR response, we set a higher stimulation rate for *protocol 2* than for *protocol 1*. The pulse width of sympathetic stimulation was set at 2 ms. The amplitude was set so that 5-Hz tonic sympathetic stimulation produced a HR increase of ~50 beats/min.

As a supplemental protocol, we performed the transfer function analysis using binary white noise signals of 0–1 Hz ($Bin_{0\text{-}1}$), 0–3 Hz ($Bin_{0\text{-}3}$), and 0–5 Hz ($Bin_{0\text{-}5}$) in a random order ($n = 5$). At least a 15-min interval was allowed between the 20-min dynamic sympathetic stimulation trials. The amplitude of sympathetic stimulation was set so that 1-Hz tonic sympathetic stimulation produced a HR increase of ~50 beats/min.

Medetomidine has higher affinity to α_2-adrenergic receptors over α_1-adrenergic receptors compared with clonidine (α_2/α_1 = 1,620:1 for medetomidine, 220:1 for clonidine) (28). However, a preliminary experiment indicated that medetomidine was not as effective as

clonidine to modulate the transfer function from dynamic sympathetic stimulation to HR. Accordingly, we examined the effects of clonidine or medetomidine on myocardial interstitial NE release in response to 5-Hz tonic stimulation (2.5 V, 2-ms pulse width) of the right cardiac sympathetic nerve in vagotomized rabbits. Two microdialysis probes were implanted in the myocardium of the left ventricular free wall. Ringer solution was perfused at 2 μl/min. After a 2-h equilibrium period, we collected 5-min dialysate samples to measure the dialysate NE concentration as an index of myocardial interstitial NE levels (14, 15). High-performance liquid chromatography with electrochemical detection was used to quantify the NE concentration. After the sympathetic stimulation was performed under the control condition, clonidine or medetomidine was intravenously administered (1.5 $mg \cdot kg^{-1} \cdot h^{-1}$). Fifteen minutes later, the sympathetic stimulation was performed under the drug administration condition. Then the drug administration was ceased. Forty-five minutes later, the sympathetic stimulation was performed under the recovery condition. We used different rabbits for clonidine and medatomidine trials. We pooled six dialysate data for statistical analysis.

Data Analysis

Data were digitized at 200 Hz utilizing a 12-bit analog-to-digital converter and stored on the hard disk of a dedicated laboratory computer system. Mean values for HR and AP during dynamic sympathetic nerve stimulation were calculated by averaging the respective data over the stimulation period.

The transfer function from dynamic sympathetic nerve stimulation to HR response was estimated by the following procedures. Twenty minutes of input data (stimulation command) and output data (HR) were resampled at 8 Hz. The resampled data were segmented into eight 50% overlapping bins consisting of 2,048 data points each. The segment length was 256 s. For each segment, the linear trend was subtracted, and a Hanning window was applied. Fast-Fourier transform was then performed to obtain the frequency spectrum of nerve stimulation rate [$N(f)$] and that of HR [$HR(f)$] (5). The power spectral density of the nerve stimulation rate [$S_{N \cdot N}(f)$], that of HR [$S_{HR \cdot HR}(f)$], as well as the cross-spectral density between these two signals [$S_{N \cdot HR}(f)$], were averaged over the eight segments. Finally, the transfer function [$H(f)$] from sympathetic nerve stimulation rate to HR response was calculated using the following equation (2, 21).

$$H(f) = \frac{S_{N \cdot HR}(f)}{S_{N \cdot N}(f)} \quad (1)$$

Transfer function parameters were determined by fitting a second-order, low-pass filter to the estimated transfer function, according to previous studies (12, 13, 23). The second-order, low-pass filter with a pure dead time [$G(f)$] is expressed as

$$G(f) = \frac{K}{1 + 2\zeta \frac{f}{f_N} j + \left(\frac{f}{f_N} j\right)^2} \exp(-2\pi f j L) \quad (2)$$

where K is a steady-state gain, f_N is natural frequency (in Hz), ζ is a damping ratio, L is pure dead time (in s), and j indicates an imaginary unit. A schematic explanation for these transfer function parameters is provided in the APPENDIX. To estimate the parameters, an iterative nonlinear least squares fitting was performed to minimize the following error function.

$$\text{error} = \frac{\sum_{k=1}^{n} |G(f) - H(f)|^2}{\sum_{i=1}^{n} |H(f)|^2}, \quad f = f_0 \times k \quad (3)$$

where f_0 is the fundamental frequency of the discrete Fourier transform, $f_0 = 1/256 = 0.004$ Hz, and k is a frequency index. The n represents the upper limit of the frequency index determined from the range of sufficient input power in the sympathetic nerve stimulation; $n = 40$, $f_0 \times n = 0.156$ Hz.

To quantify the linear dependence of the HR response on the sympathetic nerve stimulation, the magnitude-squared coherence function [$\gamma^2(f)$] was calculated by the following equation (2, 21).

$$\gamma^2(f) = \frac{|S_{N \cdot HR}(f)|^2}{S_{N \cdot N}(f) \cdot S_{HR \cdot HR}(f)} \quad (4)$$

The coherence value ranges from zero to unity. The unity coherence value indicates a perfect linear dependence between the input and output signals, whereas zero coherence indicates a total independence between the two signals.

To facilitate the intuitive understanding of the HR response to dynamic sympathetic nerve stimulation, we calculated the step response from the estimated transfer function. The step response was obtained from the time integral of the system impulse response derived from the inverse Fourier transform of the transfer function. The steady-state response was calculated by averaging the step response during the last 10 s of the 128-s response. To characterize the rising speed of the step response, the initial slope for the response was calculated as follows. An analysis of linear regression with a slope and an intercept was performed on the initial data points of the step response while varying the number of data points from 2 to 1,024. The maximum slope obtained was used as the initial slope of the response. The linear regression was performed, including the portion of the dead time. Although including the dead time reduced the maximum slope, the effect was small because the number of data points that yielded the maximum slope (~90 points) was much larger than that for the dead time (<10 points). The step response of RRI was also calculated from the corresponding transfer function from sympathetic nerve stimulation to RRI.

Statistics

All data are presented as means ± SE. In *protocol 1*, mean HR, AP, and transfer function parameters were compared before and during yohimbine administration by paired *t*-tests. In *protocol 2*, the data were compared among control, lower dose, and higher dose clonidine conditions using a repeated-measures ANOVA followed by Dunnett's test against the single control (8). In the supplemental protocol of the transfer function analysis, the data were compared among $Bin_{0\text{-}1}$, $Bin_{0\text{-}3}$, and $Bin_{0\text{-}5}$ stimulus conditions using a repeated-measures ANOVA followed by Tukey test for all pairwise comparisons. In the supplemental protocol of the NE measurement, baseline NE levels were compared before and during drug administration using a paired *t*-test. The NE levels during sympathetic stimulation were compared among control, drug administration, and recovery conditions using a repeated-measures ANOVA followed by Dunnett's test against the control condition. In all of the statistical procedures, the difference was considered significant at $P < 0.05$.

RESULTS

Figure 2*A* represents a typical recording obtained from *protocol 1*. We stimulated the cardiac sympathetic nerve according to a binary white noise signal and recorded HR response under control condition and during yohimbine administration. The presynaptic α_2-adrenergic negative feedback mechanism functioned under the control condition but not during yohimbine administration. HR changed dynamically in response to the random sympathetic nerve stimulation under both conditions. Yohimbine increased the magnitude of HR variation. The augmentation of sympathetic effect was also observed in the RRI response. Although yohimbine decreased the mean level of HR in this animal, changes in mean HR

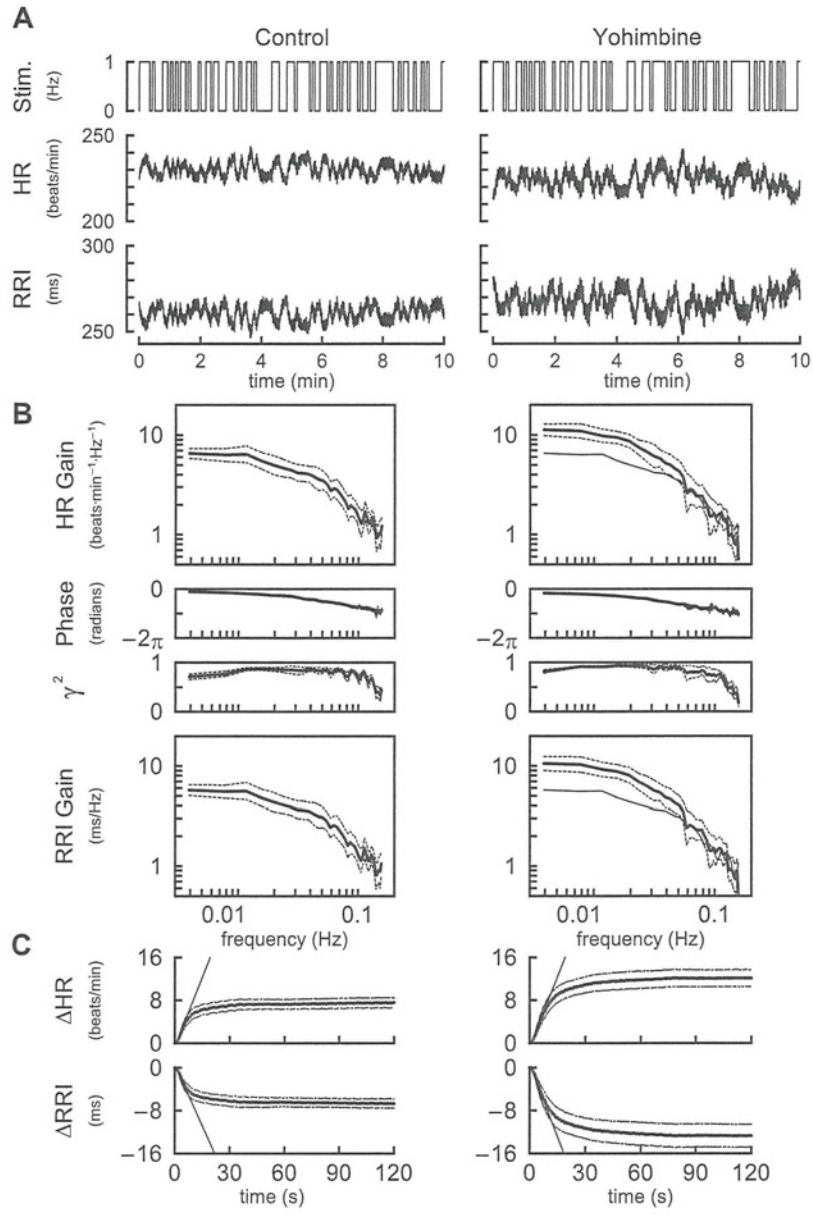

Fig. 2. *A:* representative recordings of cardiac sympathetic nerve stimulation rate (Stim; *top*), HR response (*middle*), and R-R interval (RRI) response (*bottom*) under conditions of control (*left*) and yohimbine administration (*right*) obtained in *protocol 1*. Yohimbine blocks the presynaptic α_2-adrenergic autoinhibition. The amplitude of HR variation and that of RRI variation become greater in the presence of yohimbine. *B:* transfer functions averaged over all animals in *protocol 1*. HR gain plots (*top*), phase plots (*second*), coherence functions (γ_2, *third*), and RRI gain plots (*bottom*). Yohimbine increases the dynamic gain in the frequency range between 0.004 and 0.04 Hz but not in the higher frequency range. The fine solid curve in the gain (*right*) duplicates the mean gain plot (*left*). *C:* step responses of HR (*top*) and RRI (*bottom*) calculated from the corresponding transfer functions. Yohimbine augments the steady-state response without affecting the initial slope of the response (fine oblique line). Bold, solid lines represent the mean, whereas dotted lines indicate means ± SE.

varied among the animals and were not significantly different between the control and yohimbine conditions.

Table 1 summarizes the mean HR and AP averaged from the six animals. The α_2-adrenergic blockade by yohimbine did not significantly affect the HR or AP before sympathetic nerve stimulation. Yohimbine also did not affect HR or AP significantly during the stimulation period.

Figure 2*B* illustrates the transfer functions averaged from the six animals in *protocol 1*. In the HR gain plots, the gain value was relatively constant <0.01 Hz and decreased >0.01 Hz, indicating low-pass filter characteristics of the HR response to sympathetic nerve stimulation. Yohimbine increased the HR gain from 7.1 ± 0.7 to 12.0 ± 1.7 beats·min^{-1}·Hz^{-1} at the lowest frequency of 0.004 Hz ($P < 0.05$). In contrast, yohimbine did not affect the HR gain value at 0.1 Hz (1.8 ± 0.4 vs. 1.7 ± 0.6 beats·min^{-1}·Hz^{-1}). The solid fine curve in the *right* panel duplicates the mean gain plot in the *left* panel as a reference. In the phase plots, the phase value approached zero radians at the lowest frequency and lagged with increasing frequency under both conditions. In the coherence function plots, the coherence was >0.8 in the frequency range from 0.01 to 0.08 Hz, suggesting that the HR response to sympathetic nerve stimulation in this frequency range can be explained reasonably well by linear dynamics for both conditions. Changes in the RRI gain plots were similar to those in the HR gain plots. Yohimbine increased the RRI gain from

Table 1. *Mean heart rate and arterial pressure before and during random stimulation of the cardiac sympathetic nerve*

	Control	Yohimbine
Heart rate, beats/min		
Before	259±15	244±13
During	264±15	254±17
Mean arterial pressure, mmHg		
Before	90±8	87±6
During	91±9	88±8

Values are means ± SE. Data were obtained after vagal and cardiac sympathetic nerves were cut. No statistically significant difference was detected between control vs. yohimbine values by paired *t*-tests.

6.0 ± 0.7 to 11.3 ± 1.9 ms/Hz at the lowest frequency of 0.004 ($P < 0.05$) but not at 0.1 Hz (1.8 ± 0.4 vs. 1.9 ± 0.8 ms/Hz). Given the inverse relationship between RRI and HR, the RRI phase plots (not shown) quite resembled to the corresponding HR phase plots except for the rotation by π radians.

Figure 2*C* represents the step responses of HR to sympathetic nerve stimulation calculated from the transfer functions shown in Fig. 2*B*. Yohimbine increased the steady-state response significantly (Table 2). The initial slope of the response, depicted by an oblique straight line, was not affected by yohimbine (Table 2). In the RRI step response, yohimbine augmented the steady-state response from −6.7 ± 0.9 to −12.6 ± 2.1 ms ($P < 0.05$) without affecting the initial slope (−0.71 ± 0.18 vs. −0.90 ± 0.23 ms/s).

Parameters of the transfer functions and step responses estimated in *protocol 1* are summarized in Table 2. The steady-state gain was significantly greater and the natural frequency was significantly lower in yohimbine condition compared with control. The damping coefficient and pure dead time did not differ significantly between the control and yohimbine conditions. Whereas the steady-state response was significantly increased by yohimbine, the initial slope of the step response was not significantly changed.

Figure 3*A* represents a typical recording of the sympathetic nerve stimulation and HR response obtained from *protocol 2*. The effects of α_2-adrenergic stimulation by clonidine were tested at two doses. Lower dose clonidine did not affect the magnitude of HR variation. Although lower dose clonidine decreased the mean HR in this animal, changes in the mean HR were not significantly different among the animals (Table 3). Higher dose clonidine significantly attenuated the magnitude of HR variation and also decreased mean HR. The attenuation of sympathetic effect was also observed in the RRI response during the high-dose clonidine administration.

Table 3 summarizes the mean HR and AP obtained from *protocol 2*. Higher dose, but not lower dose, clonidine significantly decreased the mean HR, both before and during cardiac sympathetic nerve stimulation. Clonidine did not affect mean AP significantly, before or during cardiac sympathetic nerve stimulation.

Figure 3*B* illustrates the transfer functions averaged from the five animals in *protocol 2*. Lower dose clonidine did not affect the transfer function significantly. In the HR gain plots, higher dose clonidine decreased the gain from 6.6 ± 0.9 to 2.7 ± 0.5 beats·min^{-1}·Hz^{-1} at the lowest frequency of 0.004 Hz ($P < 0.05$) and from 1.1 ± 0.2 to 0.5 ± 0.2 beats·min^{-1}·Hz^{-1} at the frequency of 0.1 Hz ($P < 0.05$). Higher dose clonidine did not affect the phase plot significantly. In the coherence function plots, the coherence was >0.8 in control and lower dose clonidine conditions and >0.7 in higher dose clonidine condition for the frequency range from 0.01 to 0.08 Hz, suggesting that the HR response to sympathetic nerve stimulation can be explained reasonably well by linear dynamics in all three conditions. Although relative change became smaller compared to the HR gain plots, the attenuation of transfer gain was also observed in the RRI gain plots. Higher-dose clonidine decreased the gain from 4.5 ± 0.7 to 2.8 ± 0.5 ms/Hz at the lowest frequency of 0.004 Hz ($P < 0.05$) and from 0.88 ± 0.19 to 0.04 ± 0.09 ms/Hz at the frequency of 0.1 Hz ($P < 0.05$).

Figure 3*C* represents the step responses of HR to sympathetic nerve stimulation calculated from the transfer functions shown in Fig. 3*B*. Lower dose clonidine did not affect either the steady-state response or the initial slope of the step response. In contrast, higher dose clonidine attenuated the steady-state response and also reduced the initial slope of the response. In the RRI step response, higher-dose clonidine attenuated the steady-state response from −4.9 ± 0.7 to −3.0 ± 0.6 ms ($P < 0.05$) with a significant reduction in the initial slope from −0.40 ± 0.07 to −0.23 ± 0.05 ms/s ($P < 0.05$).

Parameters of the transfer functions and step responses estimated in *protocol 2* are summarized in Table 4. The steady-state gain of the transfer function and the steady-state response of the corresponding step response were decreased by higher dose but not by lower dose clonidine. The initial slope of the step response was decreased by higher dose clonidine. The ratio of the steady-state response to the initial slope was unchanged. The natural frequency and the damping ratio of the transfer function were not affected by clonidine. The pure dead time of the transfer function was increased by lower dose, but not by higher dose, clonidine.

Figure 4*A* represents a typical recording of the sympathetic nerve stimulation and HR response obtained from the supplemental protocol. The binary white noise signals of the same sequence but different stimulus rate were applied. Increasing the stimulus rate augmented the magnitude of HR variation and increased mean HR. The increase was not proportional to the increase in the stimulus rate, however, because of the saturation of HR response to sympathetic nerve stimulation. The increase of RRI variation was not proportional to the increase in the stimulus rate either, suggesting that the saturation effect observed in the HR response was not an artifact of reciprocal relationship between RRI and HR.

Table 2. *Parameters of the transfer functions and step responses*

	Control	Yohimbine
K, beats·min^{-1}·Hz^{-1}	7.3±1.1	12.0±2.1*
f_N, Hz	0.081±0.012	0.055±0.008*
ζ	1.64±0.47	1.55±0.21
L, s	0.82±0.22	1.03±0.19
Fitting error, %	5.6±1.5	3.6±1.1
S, beats/min	7.2±0.8	12.2±1.7*
α, beats·min^{-1}·s^{-1}	0.93±0.23	0.94±0.22
S/α, s	9.1±1.4	14.4±1.9*

Values are means ± SE. K, steady-state gain; f_N, natural frequency; ζ, damping coefficient; L, pure dead time; S, steady-state response; α, initial slope; S/α, ratio of S to α. *$P < 0.05$ vs. control values.